



# Lipid nanoparticles to silence androgen receptor variants for prostate cancer therapy

Joslyn Quick<sup>a</sup>, Nancy Dos Santos<sup>b</sup>, Miffy H.Y. Cheng<sup>a</sup>, Nisha Chander<sup>a</sup>,  
Cedric A. Brimacombe<sup>a</sup>, Jayesh Kulkarni<sup>a,1</sup>, Roy van der Meel<sup>a,2</sup>, Yuen Yi C. Tam<sup>a,3</sup>,  
Dominik Witzigmann<sup>a,1</sup>, Pieter R. Cullis<sup>a,\*</sup>

<sup>a</sup> Department of Biochemistry and Molecular Biology, University of British Columbia, Vancouver, British Columbia V6T 1Z3, Canada

<sup>b</sup> BC Cancer Research Institute, 675 West 10th Avenue, Vancouver, British Columbia V5Z 1L3, Canada

## ARTICLE INFO

### Keywords:

siRNA  
Androgen receptor  
Lipid nanoparticle  
Gene therapy  
Prostate cancer  
Splice variant

## ABSTRACT

Advanced-stage prostate cancer remains an incurable disease with poor patient prognosis. There is an unmet clinical need to target androgen receptor (AR) splice variants, which are key drivers of the disease. Some AR splice variants are insensitive to conventional hormonal or androgen deprivation therapy due to loss of the androgen ligand binding domain at the C-terminus and are constitutively active. Here we explore the use of RNA interference (RNAi) to target a universally conserved region of all AR splice variants for cleavage and degradation, thereby eliminating protein level resistance mechanisms. To this end, we tested five siRNA sequences designed against exon 1 of the AR mRNA and identified several that induced potent knockdown of full-length and truncated variant ARs in the 22Rv1 human prostate cancer cell line. We then demonstrated that 2'-O methyl modification of the top candidate siRNA (siARv<sup>m</sup>) enhanced AR and AR-V7 mRNA silencing potency in both 22Rv1 and LNCaP cells, which represent two different prostate cancer models. For downstream *in vivo* delivery, we formulated siARv<sup>m</sup>-LNPs and functionally validated these *in vitro* by demonstrating knockdown of AR and AR-V7 mRNA in prostate cancer cells and loss of AR-mediated transcriptional activation of the PSA gene in both cell lines following treatment. We also observed that siARv<sup>m</sup>-LNP induced cell viability inhibition was more potent compared to LNP containing siRNA targeting full-length AR mRNA (siARf-LNP) in 22Rv1 cells as their proliferation is more dependent on AR splice variants than LNCaP and PC3 cells. The *in vivo* biodistribution of siARv<sup>m</sup>-LNPs was determined in 22Rv1 tumor-bearing mice by incorporating <sup>14</sup>C-radiolabelled DSPC in LNP formulation, and we observed a 4.4% ID/g tumor accumulation following intravenous administration. Finally, treatment of 22Rv1 tumor bearing mice with siARv<sup>m</sup>-LNP resulted in significant tumor growth inhibition and survival benefit compared to siARf-LNP or the siLUC-LNP control. To best of our knowledge, this is the first report demonstrating therapeutic effects of LNP-siRNA targeting AR splice variants in prostate cancer.

## 1. Introduction

Prostate cancer is one of the most commonly diagnosed cancers among North American men and remains a leading cause of cancer-related deaths [1,2]. Androgen deprivation therapy (ADT) is the standard treatment in the clinic due to the overactivation of the androgen receptor (AR) protein, a transcriptional regulator which is the central

driver of the disease. Despite robust responses to ADT in early-stage prostate cancer, many patients will progress to an advanced castration-resistant stage prostate cancer that is incurable [3]. Expression of constitutively active AR splice variants which are insensitive to ADT has been postulated as a key mechanism of castration-resistance in prostate cancer that hinders current AR-targeting therapies [4–6]. For example, AR-V7, the most abundantly reported AR splice variant, has a

\* Corresponding author at: Life Sciences Institute, University of British Columbia, 2350 Health Sciences Mall, Vancouver, British Columbia V6T 1Z3, Canada.  
E-mail address: [pieterc@mail.ubc.ca](mailto:pieterc@mail.ubc.ca) (P.R. Cullis).

<sup>1</sup> Current Affiliation: NanoVation Therapeutics, 2405 Wesbrook Mall, Vancouver, British Columbia, Canada V6T 1Z3.

<sup>2</sup> Current Affiliation: Laboratory of Chemical Biology, Department of Biomedical Engineering and Institute for Complex Molecular Systems, Eindhoven University of Technology, Eindhoven, The Netherlands P.O. Box 513, 5600 MB.

<sup>3</sup> Current Affiliation: Integrated Nanotherapeutics Inc., Suite 205, 4475 Wayburne Drive, Burnaby, British Columbia, Canada V5G 4X4.

truncated C-terminus and lacks an androgen ligand-binding domain (LBD) and maintains androgen-independent transcriptional activation [7]. Because ADT acts on the LBD of the AR, they are ineffective against these AR variants.

An alternative target region of the AR protein is the N-terminal domain (NTD). The NTD of the AR protein is present in all splice variants, thereby reducing the possibility of drug resistance due to target domain loss. Examples of small molecules antagonists which specifically target this domain are Sintokamide A and EPI-506, and both have shown significant antitumor activity [8–10]. A clinical trial (NCT02606123) investigating the use of EPI-506 in men with castration-resistant prostate cancer that had progressed on standard treatments of either enzalutamide or abiraterone acetate showed long-term disease stabilization at higher dose levels, indicating the potential of AR NTD targeting for clinical applications. However, the study was terminated due to the high dose burden and minor PSA declines suggesting the need for a more potent derivative [11]. Despite these setbacks, the AR NTD remains an attractive therapeutic target for the development of drugs to treat advanced-stage prostate cancer. In addition, the universally conserved presence of the NTD in all splice variants makes it an attractive target for other therapies which do not require small molecule interaction with the NTD.

More recently, methods for targeting the nucleic acid sequences which encode proteins have gained significant traction as therapeutic options. A commonly used method for this is RNA interference (RNAi), which acts at the mRNA level and is not limited in which region of the protein-encoding sequence is targeted. The effector molecules of RNAi are 21 bp small interfering RNA (siRNA), which function by entering the ubiquitous RNAi pathway; after cytosolic delivery, siRNA is processed and incorporated into the RNAi-induced silencing complex (RISC). When the siRNA-loaded RISC encounters an RNA molecule with precise complementary base-pairing with the incorporated siRNA sequence, it induces site-specific hydrolysis of the target RNA, resulting in subsequent degradation of the cleavage products via other cellular pathways [12]. Thus, essentially any region of any mRNA transcript which encodes a protein can be used as a therapeutic target to eliminate translation of the offending protein [13]. There are clear potential advantages of siRNA over the use of small-molecule therapies for targeting AR splice variants because universally conserved regions of spliced transcripts can be targeted, removing potential for development of the resistance mechanism described above. Because siRNA targeting is highly sequence specific, there is a unique opportunity to address the issue with protein domain binding by using sequence-specific gene knockdown of AR transcripts. To successfully deliver siRNA as a cancer therapy, a specialized siRNA delivery vehicle is required as naked siRNA rapidly degrades in circulation prior to delivery to target cells or is degraded within endosomes [12].

Lipid nanoparticles (LNPs) are nanoscale (<100 nm) lipid structures used to encapsulate siRNA and other payloads; encapsulated siRNA has vastly improved stability and transfection capability under physiological conditions which allows for delivery of the siRNA payload to distal tumor sites upon systemic administration. These LNP platforms also facilitate intracellular trafficking and enable escape from endosomal compartments, thereby enhancing the overall therapeutic efficacy [14]. The success of the FDA approved Onpatro® LNP-siRNA for the treatment of transthyretin-induced amyloidosis [15–17] provided a clinical demonstration of LNP utility in siRNA delivery, and LNPs are currently the one of the most widely used functional vectors for siRNA delivery *in vivo*. Although the preferential accumulation of siRNA-LNP in the liver is a major obstacle for delivery to other tissues, a series of siRNA-LNPs formulation have shown efficacy in various prostate cancer models with repeat dosing, a higher PEG lipid content, and use of a more stably retained PEG lipid to improve the biodistribution of LNP systems to the tumor site [18–20].

In this study, we identified an siRNA sequence that induces effective silencing of AR splice variants and improved its functionality through a

2'O methyl modification (siARv<sup>m</sup>). This was followed by formulating siARv<sup>m</sup>-LNP that induced significant knockdown of AR transcripts and AR-mediated prostate-specific antigen (PSA) levels in two different prostate cancer cells lines (22Rv1 and LNCaP) with varying degrees of expression and dependency on AR, AR-V7 and PSA genes. siARv<sup>m</sup>-LNP showed inhibitory effects on a broad AR population, as well as a functional AR-dependent reduction in 22Rv1 and LNCaP cell viability. LNP-siARv<sup>m</sup>-LNP biodistribution was determined in a 22Rv1 xenograft mouse model using <sup>14</sup>C-labelled DSPC, where major radiodisposition was observed in the liver and spleen (14% and 11% ID/g, respectively), with ~4.4% ID/g of radioactivity found in tumors. Repeat administration of LNP-siARv<sup>m</sup> successfully slowed tumor progression and increased survival of 22Rv1 tumor-bearing mice. Taken together, these results demonstrate the potential use of LNP-siARv<sup>m</sup> as a treatment strategy for advanced castration-resistant prostate cancers.

## 2. Materials and methods

### 2.1. Materials

1-stearoyl-2-oleoyl-sn-glycero-3-phosphocholine (DSPC) was purchased from Avanti Polar Lipids (Alabaster, AL), cholesterol was obtained from Sigma-Aldrich (St. Louis, MO), and heptatriacontanoic acid (7:28,31-tetraen-19-yl 4-(dimethylamino) butanoate (DLin-MC3-DMA) was obtained from Biofine International (Vancouver, BC, Canada). (R)-2,3-bis(octadecyloxy)propan-1-yl (methoxy polyethylene glycol 2000) carbamate (PEG-DMG) was synthesized as previously described by Akinc et al. [21]. 1,2-Distearoyl-rac-glycero-3-methylpolyoxyethylene (PEG-DSG) was a generous from Alnylam Pharmaceuticals (Cambridge, MA, USA).

### 2.2. Cell culture

All cell lines used were obtained from the American Type Culture Collection (Manassas, VA). 22Rv1 and LNCaP cells were maintained in RPMI-1640 medium supplemented with 10% (v/v) fetal bovine serum (FBS). PC3 cells were grown in Dulbecco's Modified Eagle Medium supplemented with 10% FBS. All cell lines were incubated at 37 °C in a 5% CO<sub>2</sub> environment. All cell culture media and reagents were obtained from Gibco (Thermo Fisher Scientific, Valencia, CA).

### 2.3. Quantitative reverse transcription-PCR

Total RNA was extracted using a PureLink® RNA Mini Kit (ThermoFisher Scientific Inc., Valencia, CA) according to the manufacturer's instructions. A NanoDrop™ Lite Spectrophotometer (ThermoFisher Scientific Inc.) was used to determine RNA concentration. 1 µg of total RNA was used as template for cDNA synthesis using a High-Capacity cDNA Reverse Transcription Kit (Applied Biosystems, Foster City, CA). Quantitative real time-PCR (qRT-PCR) was performed using TaqMan® Fast Advanced Master Mix (Applied Biosystems) and primers purchased from Integrated DNA Technologies (IDT, Coralville, IA; described in Supplementary Table S1). A Step One Plus Real-Time PCR System (Applied Biosystems) was used to perform all qRT-PCR experiments. The β-actin gene (ACTB) was utilized as an endogenous reference against which RNA expression levels were standardized. For relative gene expression, target mRNA levels were normalized to β-actin mRNA levels using the delta CT (CT = cycle threshold) method and the following formula: 2<sup>-ΔCT</sup> where ΔCT = target gene CT – β-actin CT.

### 2.4. Gene silencing

All screening siRNA molecules were purchased from IDT and were designed as 25/27-nucleotide RNA duplexes (Dicer-substrate siRNA). Non-modified screening siRNAs are described in Supplementary Table S2. The modified siARv had the following sequence: sense, 5'-

ccAuGcAACUCcUuCaGcAACAGcdA-3'; antisense, 5'-UGcUGUUGcUgAaGGAGUUGCAuGgug-3'. The siRNA targeting exon 8 of the AR mRNA (siARf1) was obtained from Alnylam® Pharmaceuticals and had the following sequence: sense, 5'-cuGGGAAAGucAAGcccAudTsdT-3'; antisense, 5'-AUGGGCUUGACUUCCcAGdTsdT-3'. An siRNA targeted against luciferase (siLUC; sense, 5'-cuuAcGcuGAGuAcuucGAdTsdT-3'; antisense, 5'-UCGAAGuACuACGCGuAAGdTsdT-3') served as a negative control. Lower case letters indicate 2'-O-methyl modification and "s" indicates phosphorothioate RNAs. For siRNA screening studies, 22Rv1 cells were seeded in a 24-well plate overnight and treated with the indicated siRNAs using Lipofectamine® RNAiMAX (ThermoFisher Scientific Inc., Valencia, CA), following the manufacturer's transfection procedure. At the end of the treatment (24 h), cells were lysed for RNA purification and qRT-PCR analysis, as described above. For gene knockdown studies, 22Rv1 or LNCaP cells were seeded overnight in 24-well plates and treated with siRNA-LNP at 0.1 µg/mL siRNA for 24 h (AR knockdown) or 48 h (PSA knockdown). For gene knockdown studies, the delta-delta CT method was utilized to calculate relative expression of target mRNAs against a control reference sample.

## 2.5. Western blot analysis

Cell protein extracts were resolved on SDS-PAGE and proteins were transferred to PVDF membranes. After blocking at room temperature in 5% milk in PBS/0.1% Tween-20, membranes were incubated overnight at 4 °C with the indicated primary antibodies and dilutions: AR N-terminus (SC-7305, Santa Cruz Biotechnology, Santa Cruz, CA) at 1:500; AR-V7 (ab198394; Abcam) at 1:500; β-actin (ab8227, Abcam) at 1:5000. β-actin was used as the loading control. Following secondary antibody incubation, antigen-antibody complexes were detected using Millipore Immobilon Western Chemiluminescent HRP Substrate (Billerica, MA, USA).

## 2.6. Preparation of siRNA-LNPs

LNPs were prepared as previously described [15]. Lipids were dissolved in ethanol and mixed together at a molar ratio of 50/10/38.5/1.5 ionizable amino-lipid DLin-MC3-DMA, phospholipid (DSPC), cholesterol, and PEG-DMG, respectively. For *in vivo* studies, LNP were prepared using 2.5 mol% PEG-DSG. Appropriate volumes of lipid were mixed with siRNA dissolved in 25 mM sodium acetate pH 4 using a microfluidic chip (Precision Nanosystems, Vancouver, BC) or T-junction mixer and a dual-syringe pump (Harvard Apparatus, Holliston, MA) at a volumetric ratio of 3:1 lipid:siRNA. The siRNA-LNP systems were then dialyzed twice against 1× phosphate-buffered saline (PBS) pH 7.4 (GIBCO, Carlsbad, CA) using Spectro/Por dialysis membranes (molecular weight cut-off 12,000–14,000 Da, Spectrum Laboratories, Rancho Dominguez, CA). For the biodistribution study requiring radiolabeled LNP, [<sup>14</sup>C]-DSPC (American Radiolabeled Chemicals, Saint Louis, MO) was incorporated at a ratio of 0.04 µCi/µmol total lipid.

## 2.7. Analysis of siRNA-LNP

The size and PDI of LNPs were determined by dynamic light scattering (DLS; number mode, Malvern Zetasizer Nano ZS, Worcestershire, UK). Total siRNA concentration and siRNA encapsulation was determined by absorbance at 260 nm and by use of the Quant-iT™ Ribo-Green™ RNA Assay (Invitrogen). Lipid concentration was determined by measurement of cholesterol content using a Cholesterol E enzymatic assay (Wako Chemicals USA, Richmond, VA).

## 2.8. Cell viability assays

The viability of prostate cancer cells treated with siRNA-LNP was measured using the 3-(4,5-dimethyl-2-thiazolyl)-2,5-diphenyl-2H-tetrazolium bromide (MTT) assay (Sigma-Aldrich, St. Louis, MO), as

described previously [22]. Briefly, cells (22Rv1, LNCaP or PC3) were seeded in 96-well plates, grown overnight, and then treated for 96 h with siARv<sup>m</sup>-LNP, siARf1-LNP, or siLUC-LNP at the indicated siRNA concentrations. After 96 h, 25 µL of a 5 mg/mL solution of MTT reagent in PBS was added to cells without aspirating cell media. After a 2-h incubation at 37°C, 100 µL of 20% SDS (w/v) dissolved in 50% DMF was added to each well. The absorbance was measured at 570 nm, and values were compared to untreated control to obtain "% cell viability". The proliferation of 22Rv1 cells treated with siRNA-LNP was determined from attached cell count by Hoechst 33342 staining. Cells were seeded in 96-well plates, grown overnight, and then treated with siARv<sup>m</sup>-LNP, siARf1-LNP, or siLUC-LNP at 1.0 µg/mL siRNA. 100 µL of pre-warmed cell media containing 0.6 µg/mL Hoechst 33342 was added directly to wells at the end of the treatment. Plates were incubated at 37 °C for 30 min, then scanned using the Cellomics Arrayscan VTI automated fluorescence imager. The cells were imaged with a 20× objective with the Hoechst channel, and data was collected from 10 fields per well, with three wells per treatment group. A nuclear mask generated by the Cellomics Compartmental Analysis software from the Hoechst stain was used to quantitate cell number. The cell numbers for each treatment were compared to untreated control to obtain "% cell number".

## 2.9. Biodistribution study

Male NRG mice were obtained from ARC at 6–10 weeks of age. After 1 week of adaptation, mice were inoculated subcutaneously with 2 × 10<sup>6</sup> 22Rv1 cells suspended in 50% Matrigel on the lower back under isoflurane anesthesia. When tumor size reached 250 mm<sup>3</sup>, siARv<sup>m</sup>-LNP containing trace amounts of [<sup>14</sup>C]-DSPC were administered by a single injection of 5 mg/kg (siRNA/body weight) into the lateral tail vein at an injection volume of 10 µL/g mouse. At 24 h, the mice were anesthetized with CO<sub>2</sub> and blood withdrawn by cardiac puncture for collection in microtainer tubes with EDTA (Becton-Dickinson, Franklin Lakes, NJ). A portion of the blood was centrifuged at 500 g for 10 min to isolate plasma. Tumor and organ tissues were processed by transferring the pre-weighed whole organs (or a piece of the liver, 40–60mg) to Fastprep tubes and homogenized in PBS (0.75–1 mL) using a Fastprep-24 (MP Biomedical, Santa Ana, CA). Aliquots (0.1–0.2 mL of the homogenate and plasma were transferred to 7 mL glass scintillation vials and subjected to a digestion and decolorization protocol as previously described [22]. Radioactivity was measured using a Beckman Coulter LS 6500 liquid scintillation counter (Mississauga, Ontario, Canada). The percent recovery in blood was calculated based on a blood volume of 70 mL/kg animal weight. Tumor and organ associated radioactivity are expressed as percent injected dose per total organ weight.

## 2.10. Therapeutic efficacy study

Male NRG mice were inoculated with 22Rv1 cells as described above. When tumor size reached 100 mm<sup>3</sup>, mice were randomly assigned to PBS control or 5 mg/kg siARv-LNP, siARf1-LNP or siLUC-LNP (10–11 mice per group). Mice were treated i.v. through the lateral tail vein once daily for 3 days and then twice per week thereafter. Surviving mice were sacrificed on day 20 and tumors were harvested for evaluation of mRNA expression by qRT-PCR.

## 2.11. RNA isolation from xenograft tissue

A piece of each tumor tissue was homogenized in 0.75 mL TRIzol reagent (Thermo Fisher Scientific) using a Fastprep-24 instrument, following which RNA was isolated from the homogenized samples following the TRIzol reagent procedural guidelines. A NanoDrop™ Lite Spectrophotometer was used to determine total RNA concentrations, and 1 µg of total RNA was used as template for cDNA synthesis, and qPCR experiments were carried out as described earlier.

## 2.12. Statistical analysis

One-way ANOVA was applied to compare tumor volumes at each time-point between PBS control and the other treatment groups. The Log-rank test was applied to analyze survival data. Levels of statistical significance were set at  $P < 0.05$ .

## 3. Results

### 3.1. AR, AR-V7 and PSA expression in prostate cancer cell lines

Our overarching objective was to develop a ubiquitous siRNA-LNP system targeting all AR variants (Fig. 1A–C). Therefore, we sought to study prostate cancer cells with varying molecular phenotypes. Previous studies indicate that the 22Rv1 and LNCaP cell lines exhibit varying degrees of expression and dependency for the AR, AR-V7 (the AR splice variant composed of exons 1–3 and a cryptic 3' exon), and prostate-specific antigen (PSA) genes [7,23–25]. We confirmed these reports by measuring the relative levels of AR and AR-V7 mRNA using RT-qPCR. When compared against  $\beta$ -actin mRNA levels the 22Rv1 cell line had relatively high endogenous levels of the AR, AR-V7 and PSA mRNA (Fig. 1D), potentially contributed to by repeat of exon 3 in the AR gene. Comparatively, the LNCaP cell line expressed high levels of AR and PSA mRNA, but extremely low levels of AR-V7 transcripts (Fig. 1E). The use of these two prostate cancer cell lines with opposing levels of AR splice variant expression and dependence enabled us to investigate the siRNA-LNP's gene silencing efficacy, while mimicking the variation in AR status and prostate cancer phenotypes.

### 3.2. siRNA sequence screen for effective ARs mRNA knockdown in 22Rv1 cells

A total of five siRNA sequences (siARv, siARv- $\beta$ , siARv- $\gamma$ , siARv- $\delta$ , or siARv- $\epsilon$ ) were designed to target AR exon 1 (Fig. 2A and Table S2) and were tested by *in vitro* transfection into 22Rv1 cells using a commercial Lipofectamine™ formulation as an initial screening method. The relative knockdown efficiencies of the siRNA sequences were measured by RT-qPCR. We found that transfection of all five siRNAs resulted in reduced mRNA levels of both AR and AR-V7 relative to the untreated cells and siLUC negative control. The fact that all siRNAs which targeted AR exon 1 produced a similar trend in mRNA knockdown supported that the knockdown of AR transcript levels was a specific RNAi-induced effect. We further investigated the selective transfection potency of siARfl, an siRNA designed against exon 8 of the AR gene, which had minimum silencing capacity against the AR-V7 mRNA in 22Rv1 cells (Fig. 2B). Of these five siRNA sequences, we identified siARv to be the most potent, (>80% knockdown). To further enhance its function, we proceeded to chemically modify this siRNA to enhance stability and prevent activation of the innate immune system [26,27]. A 2'-O-methyl modification was introduced into the siARv sequence, generating 2'-O-methylated siARv (siARv<sup>m</sup>). The transfection and gene silencing potency of siARv<sup>m</sup> were then compared to control siRNA (siARfl and siLUC) in 22Rv1 cells. The siARv<sup>m</sup> sequence retained its silencing activity after the modification (~70% AR mRNA knockdown and ~85% AR-V7 mRNA knockdown relative to untreated cells), confirming that chemical alteration did not compromise its activity (Fig. 2C).

The protein levels of full-length AR, AR variants, and AR-V7 protein were also investigated after treatment with all previously examined

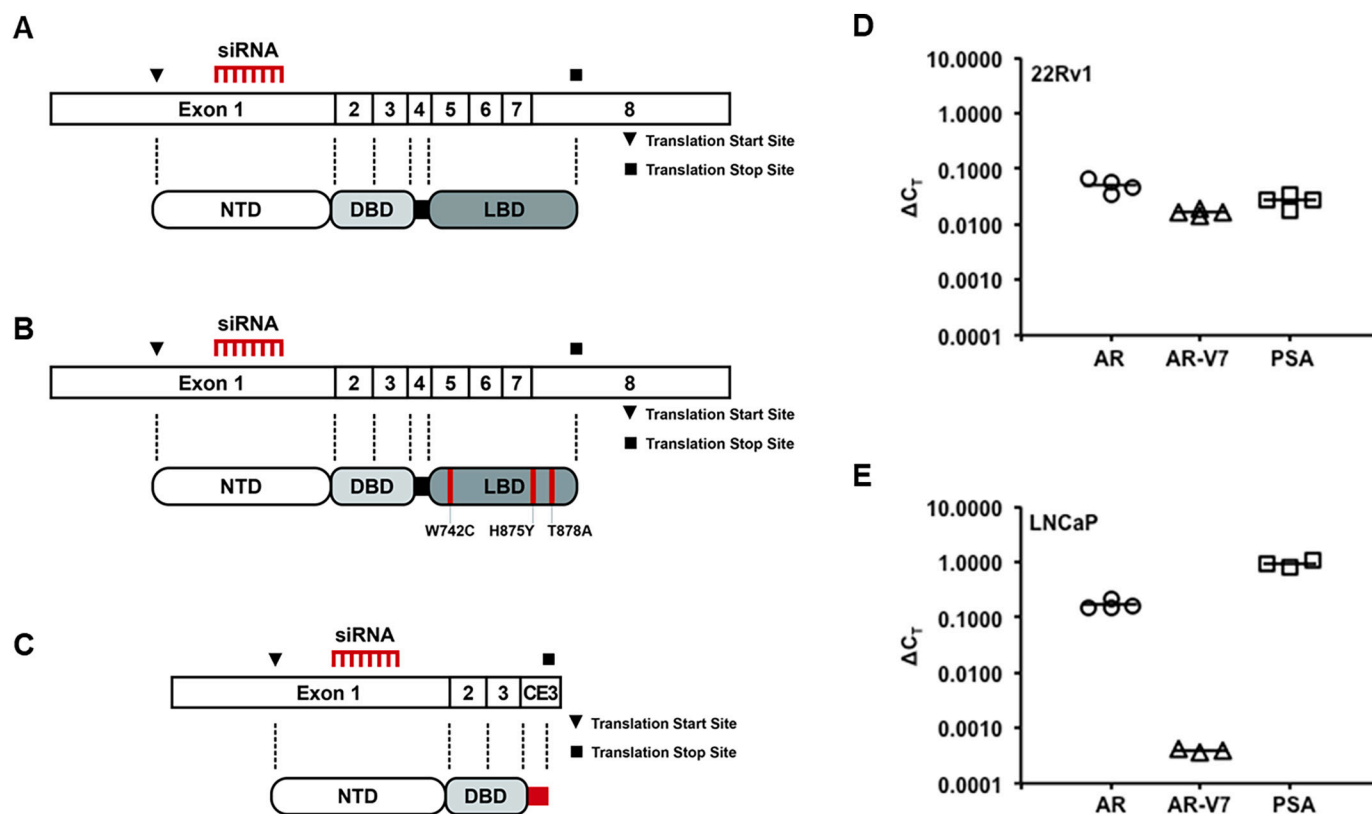


**Fig. 1.** Targeting exon 1 of androgen receptor mRNA with siRNA and the relative gene expression levels of AR, AR-V7, and PSA in prostate cancer cell culture models. Schematic representation of full-length AR mRNA and protein domains (A), AR with mutations in the LBD that confer promiscuous steroid signaling and anti-androgen antagonism (B), and constitutively active AR splice variants that completely lack the LBD such as AR-V7 (C). (D) Relative mRNA levels of WT AR, AR-V7, and PSA in the 22Rv1 cell line as measured by RT-qPCR; levels were normalized to that of  $\beta$ -actin and are represented as the  $\Delta C_T$  value. (E) Relative mRNA levels of WT AR, AR-V7, and PSA in the LNCaP cell line as measured by RT-qPCR; levels were normalized to that of  $\beta$ -actin and are represented as the  $\Delta C_T$  value. Mean values are represented by the horizontal bars;  $n \geq 3$ .



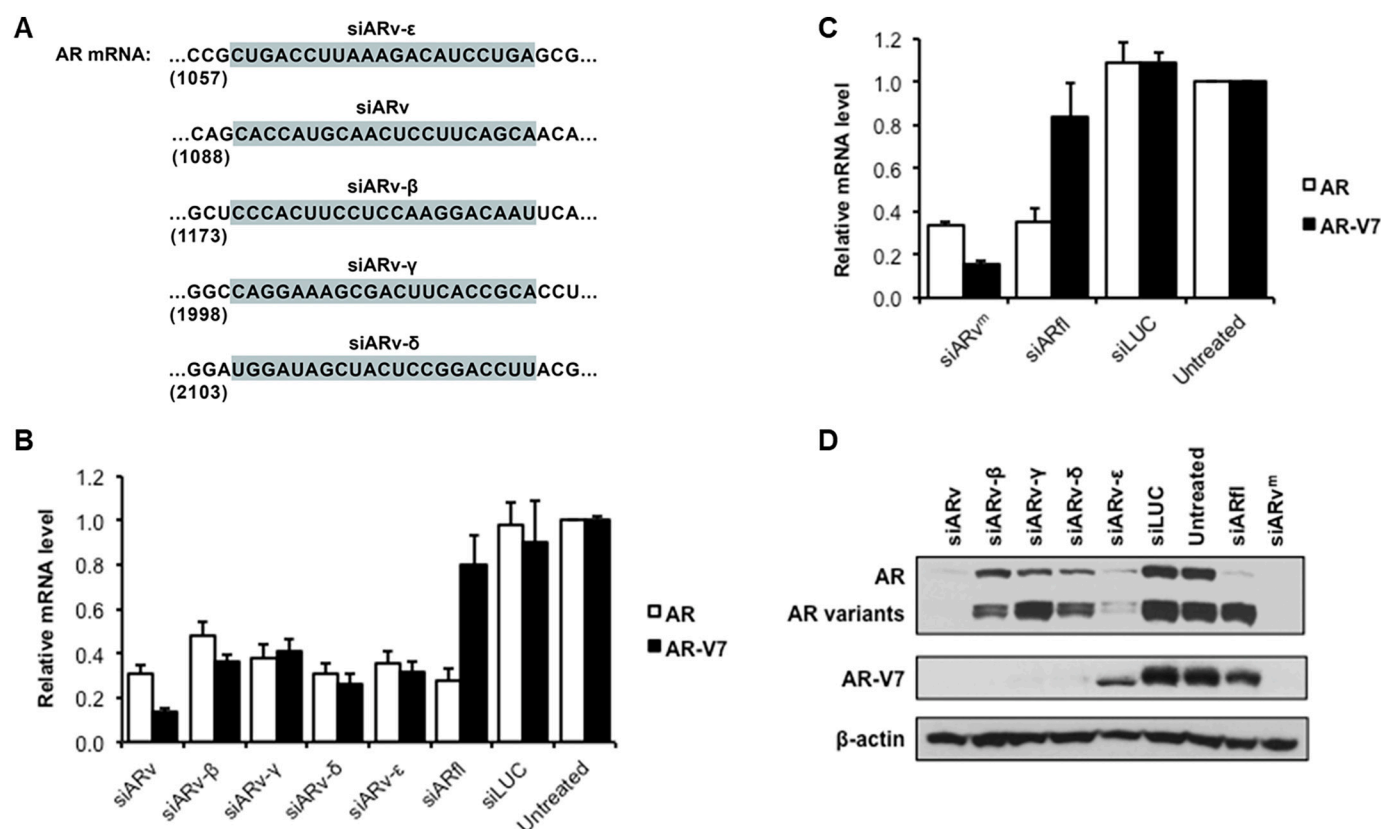


**Fig. 2.** Screening active siRNAs targeting AR variants in 22Rv1 cells. (A) Nucleic acid sequence of each tested siRNA within the AR mRNA (Accession number: NM\_000044). (B) Relative mRNA levels in 22Rv1 cells 24 h post-transfection with siRNA targeted against exon 1 of the AR mRNA (siARv, siARv-β, siARv-γ, siARv-δ, or siARv-ε) compared to siRNA targeting the AR LBD (siARf1) and negative control siRNA complementary to the luciferase gene (siLUC), as measured by RT-qPCR and normalized to β-actin. Data represents mean ± SD;  $n = 4$ . (C) Relative AR mRNA levels in 22Rv1 cells transfected with 2′-O-methylated siARv against siARf1 and siLUC control, normalized to β-actin. Data represents mean ± SD;  $n = 3$ . (D) Western blots of 22Rv1 cell lysates prepared 48 h post-transfection to detect full-length AR, variant AR (by the AR N-terminus antibody), and AR-V7 expression (by the AR-V7-specific antibody). β-actin was used as a loading control.

siRNAs. The 22Rv1 cells were treated with 10 nM of siRNA in the Lipofectamine™ formulation for 48 h. All three AR protein levels were significantly reduced when treated with the siARv<sup>m</sup> as shown in the western blot analysis (Fig. 2D), while AR variants, and AR-V7 protein expression was not reduced in siARf1 treated cells. The specific siARv<sup>m</sup> induced AR variants, and AR-V7 protein reduction correlated with the overall decrease of the corresponding mRNA levels. Both mRNA and protein expression studies showed that the siARv<sup>m</sup> sequence was the most potent sequence even after modification, therefore, this optimized lead sequence was used for all subsequent studies.

### 3.3. siARv<sup>m</sup>-LNP formulation and ARs and PSA mRNA knockdown in 22Rv1 and LNCaP cells

Once the siARv<sup>m</sup> molecule was identified through small-scale screening efforts using Lipofectamine™, it was formulated into LNP systems to confirm the knockdown efficiency and cell viability in both 22Rv1 and LNCaP cells. LNPs utilized for all *in vitro* studies were formulated with 50 mol% DLin-MC3-DMA (ionizable lipid), 1.5 mol% PEG-DMG, 38.5 mol% cholesterol and 10 mol% DSPC using the rapid mixing method described by Jayaraman et al. [15]. As depicted from the cryo-EM, the siARv<sup>m</sup>-LNP had a size of  $50 \pm 10$  nm and exhibited an electron-dense core structure containing siRNA and ionizable lipid (Fig. S1A). The apparent size of the siARv<sup>m</sup>-LNP system agreed with measurements from DLS, with a reported hydrodynamic radius of  $56 \pm 1$  nm (Fig. S1B). Similarly, the other siRNA-LNP controls such as siARf1-LNP and siLUC-LNP were also fabricated using the same formulation and were found to exhibit similar characteristic.

Next, the 22Rv1 and LNCaP cell lines were treated with 0.1 μg/mL

siRNA-LNP for 24 h and assayed for the effects on gene expression. siARv<sup>m</sup>-LNPs mediated specific knockdown of AR and AR-V7 in both cell lines showed 80–90% reduction in mRNA levels relative to the untreated control. Whereas treatment with siARf1-LNP only showed knockdown of AR mRNA, while the negative control siLUC-LNP showed no AR or AR-V7 mRNAs knockdown. This further demonstrates the functionality of the siARv<sup>m</sup> encapsulated in the LNP carrier against both the AR and AR-variant mRNA (Fig. 3A).

Transcription of the PSA gene is androgen regulated via the AR. The promoter of the PSA gene includes several AR binding sites which when bound, promote transcription of PSA mRNA [25]. The truncated AR-V7 variant retains transcriptional activation activity of the PSA promoter, thus PSA levels serve as an indicator for AR activity [28,29]. Therefore, we investigated whether treatment with siARv<sup>m</sup>-LNP exerts an inhibitory effect of AR transcriptional activation in 22Rv1 and LNCaP cells. Treatment with 0.1 μg/mL siARv<sup>m</sup>-LNP for 48 h showed a 50% and 70% reduction in PSA expression compared to the untreated control in 22Rv1 and LNCaP cell lines, respectively, whereas siARf1-LNP was only effective in reducing relative PSA mRNA levels in LNCaP cells (Fig. 3B). This data indicated that siARv<sup>m</sup>-LNPs are capable of inhibiting both PSA mRNA transcription and upstream AR signaling in prostate cancer cells expressing either WT and/or the AR-V7 variant, demonstrating the potential for targeting of this androgen-insensitive AR variant.

### 3.4. RNAi induced therapeutic efficacy of siARv<sup>m</sup>-LNP in androgen dependent and sensitive prostate cancer cells

After validating the siARv<sup>m</sup>-LNP system for knockdown of AR variants mRNA and subsequent AR-mediated transcriptional activation of

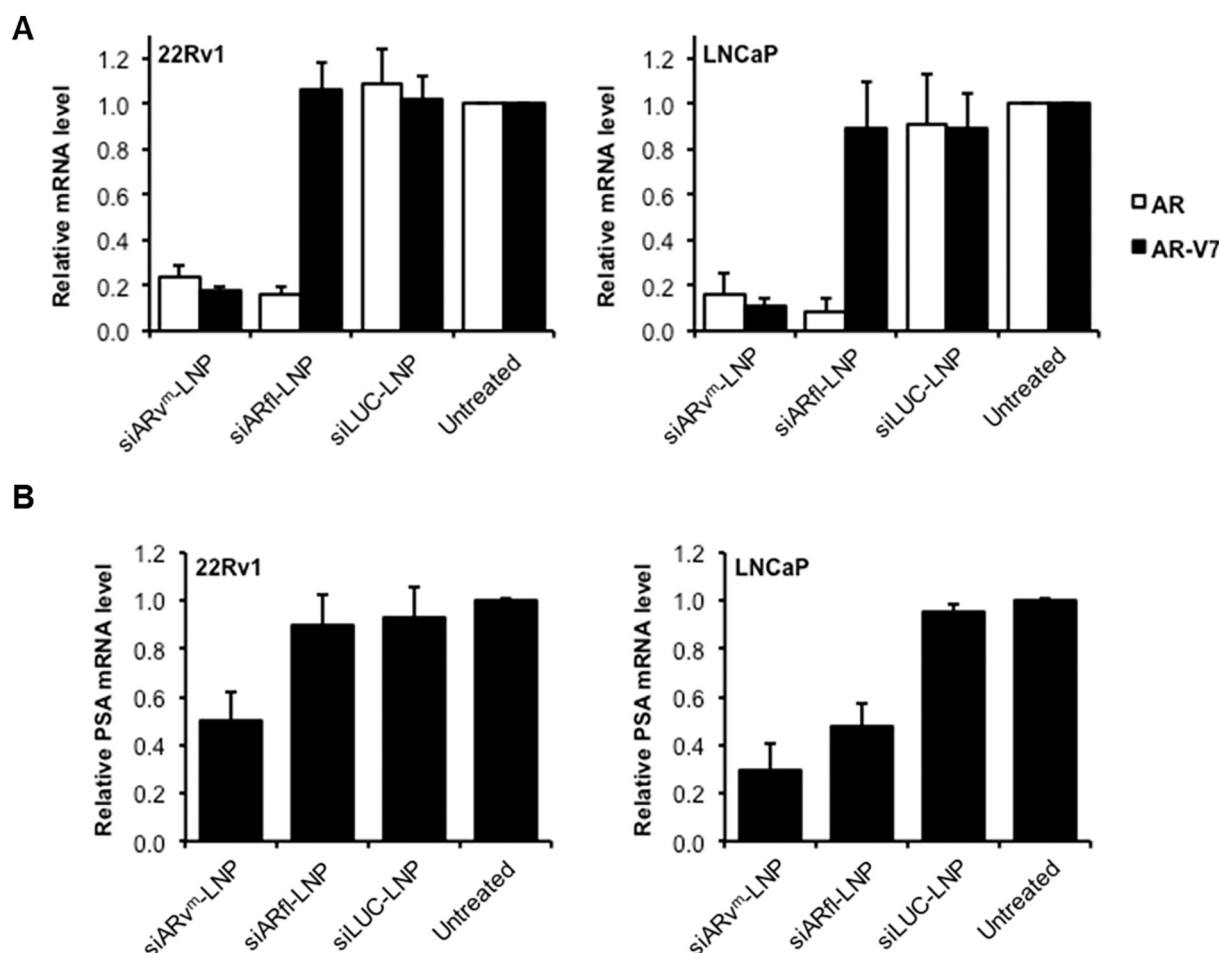


**Fig. 3.** siARv<sup>m</sup>-LNP mediated *in vitro* knockdown of AR and AR-V7 mRNA and decreases PSA mRNA expression levels in both 22Rv1 and LNCaP cells. AR and AR-V7 mRNA expression levels were quantified in (A) 22Rv1 and LNCaP cells following treatment with 0.1  $\mu\text{g/mL}$  siARv<sup>m</sup>-LNP, siARfl-LNP, or siLUC-LNP for 24 h. Expression was normalized to the  $\beta$ -actin gene. Data represents mean  $\pm$  SD;  $n = 3$ . PSA mRNA expression levels were detected in (B) 22Rv1 and LNCaP following treatment with 0.1  $\mu\text{g/mL}$  siARv<sup>m</sup>-LNP, siARfl-LNP, or siLUC-LNP for 48 h. Expression was normalized to the  $\beta$ -actin gene. Data represents mean  $\pm$  SD;  $n = 3$ .

target genes, we tested the effect of siRNA-LNPs had on cell viability using three prostate cancer cells with varying androgen-dependence (22Rv1 - androgen-dependent, LNCaP - androgen-sensitive, PC3-androgen-independent). LNP containing siARv<sup>m</sup>, siARfl, or siLUC were incubated with cells over a dose range of 0.1–10  $\mu\text{g/mL}$  for 96 h. At a dose of 1  $\mu\text{g/mL}$ , siARv<sup>m</sup>-LNP reduced cell viability by 60% and 40% in 22Rv1 and LNCaP cells, respectively (Fig. 4A and B). Notably, the siARv<sup>m</sup>-LNP showed higher RNAi-induced toxicity compared to siARfl-LNP in 22Rv1 cells (Fig. 4A) whereas in LNCaP cells, there was no significant cell viability difference between the siARv<sup>m</sup>-LNP and siARfl-LNP (Fig. 4B) which suggested that the significantly reduced AR-V7s mRNA was strongly associated with the cell viability for the 22Rv1 cell line. These results indicated that the targeting of exon 1 of the AR gene had knocked down both full-length and variant AR and was effective across prostate cancer cell lines with different AR expression profiles. It also demonstrated that knockdown of full-length AR alone with the siARfl-LNP system and antagonizing full-length AR signaling was ineffective against prostate cancer with high expression of AR splice variants. Consistent with the siARv<sup>m</sup> specificity for AR mRNA, siARv<sup>m</sup>-LNP had no effect on the viability of PC3 cells, as the viability of PC3 is not dependent on functional ARs (Fig. 4C). Similarly, treatment with siARfl-LNPs and negative control siLUC-LNPs did not affect cell viability in the androgen-independent PC3 cells. Overall, non-specific siRNA-LNP toxicity was only observed with the 22Rv1 cells treated at the highest dose (10  $\mu\text{g/mL}$ ), which suggested the cell lines might exhibit hypersensitivity toward the siRNA used in this study.

The effect of siARv<sup>m</sup>-LNP on 22Rv1 cell viability was also visualized and confirmed by high throughput fluorescence cell counting. After treatment with siRNA-LNPs at 1.0  $\mu\text{g/mL}$  for 96 h, live cells were stained with Hoechst dye, and the cell number was counted through an automated fluorescence imager. Treatment with siARv<sup>m</sup>-LNP showed a significant reduction in 22Rv1 cell number to around 55% in comparison to siARfl-LNP, siLUC-LNP, and the untreated control where no apparent cell death was observed (>90%) (Fig. S2A). 22Rv1 cells also exhibited a higher degree of morphological changes in the nuclei typical of apoptosis (condensed and fragmented nuclei), as indicated in Fig. S2B. These observations provide additional support for the concept that the siARv<sup>m</sup>-LNP system reduced cell viability of prostate cancers with both full-length AR and variant AR expression that was androgen-dependency. We propose that the siARv<sup>m</sup>-LNP system may prove more potent toward prostate cancer treatment than siRNA systems that only target full-length AR splices mRNA.

### 3.5. Biodistribution of siARv<sup>m</sup>-LNP in mice bearing 22Rv1 xenografts

Prior to investigating the *in vivo* efficacy of the siARv<sup>m</sup>-LNP system, the biodistribution was determined by the addition of trace amounts of [<sup>14</sup>C]-radiolabeled DSPC into the siARv<sup>m</sup>-LNP. Previous studies in our lab have demonstrated that the dissociation rate of DSPC from systems of similar size is <1% per hour in mouse plasma, making the [<sup>14</sup>C]-DSPC a viable LNP tracker lipid [22]. To increase circulation lifetime for the siARv<sup>m</sup>-LNPs [30] and improve *in vivo* gene silencing potency [22], the

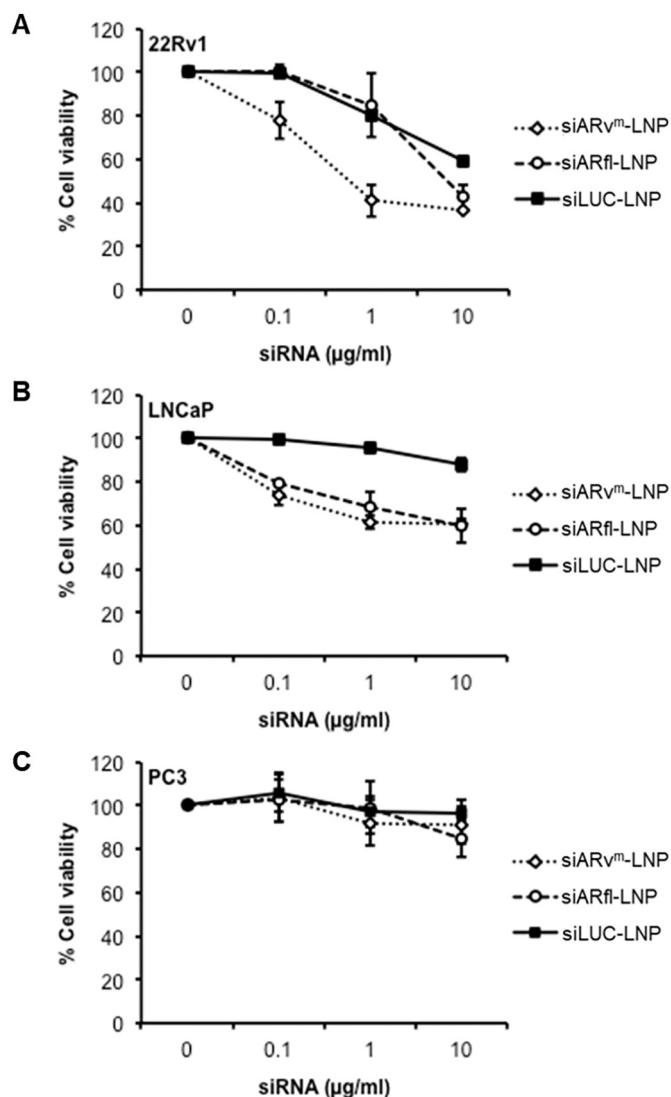


**Fig. 4.** Treatment with siARv<sup>m</sup>-LNP reduces the cell viability of both 22Rv1 and LNCaP cell lines measured by MTT assay. MTT assay was used to evaluate effects of siARv<sup>m</sup>-LNP, siARfl-LNP, and siLUC-LNP on viability in (A) 22Rv1 (AR-dependent), (B) LNCaP (AR-sensitive), and (C) PC3 cells (AR-independent) following a 96-h treatment. % Cell viability was expressed as a percentage absorbance at 570 nm relative to the untreated control cells. Data represents mean  $\pm$  SD;  $n = 3$ .

PEG lipid anchor and concentration for all of the LNP systems used *in vivo* was replaced from 1.5 mol% PEG-DMG to 2.5 mol% PEG-DSG. Subcutaneous 22Rv1 tumor-bearing mice were intravenously (*i.v.*) injected with 5 mg/kg siARv<sup>m</sup>-LNP once tumors reached a size of 250 mm<sup>3</sup>. After 24 h of treatment, the accumulation of radiolabeled LNPs in tumor, blood, liver, spleen, kidney, heart, and lung were measured through *ex vivo* gamma counting (Fig. 5). The percentage of injected radiolabel dose per gram (%ID/g) of tissue in the blood, kidney, heart, and lung were between 1.2 and 3.6% ID/g, with a significant proportion of the siARv<sup>m</sup>-LNP accumulated in the liver and spleen (14 and 11% ID/g, respectively). About 4.4% %ID/g of the siARv<sup>m</sup>-LNP was accumulated at the tumor site, corresponding to  $\sim 6 \mu\text{g}$  siRNA per gram tissue. The biodistribution results inferred that the optimized siARv<sup>m</sup>-LNP formulation had effectively delivered the siARv<sup>m</sup> payload to the distal 22Rv1 tumor site.

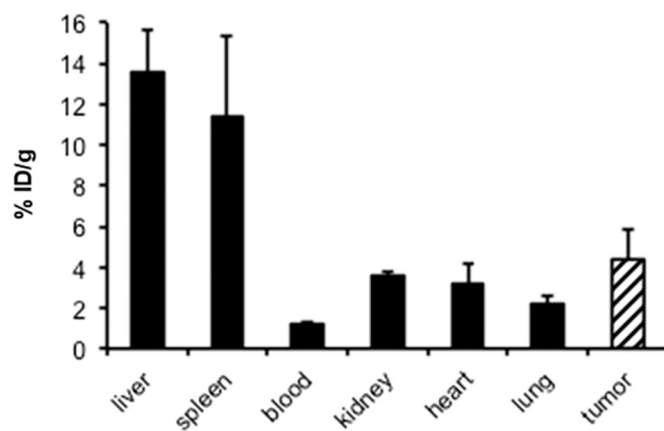


**Fig. 5.** Biodistribution of siARv<sup>m</sup>-LNP in mice bearing 22Rv1 xenograft tumors. Mice were inoculated subcutaneously with 22Rv1 cells. Once tumors reached 250 mm<sup>3</sup>, mice were injected with 5 mg/kg siARv<sup>m</sup>-LNP labelled with the lipid tracer [<sup>14</sup>C] DSPC. At 24 h post-injection, plasma, tumors, and organs were counted for <sup>14</sup>C labelled DSPC in a scintillation counter. The percent recovery in blood was calculated based on a blood volume of 70 mL/kg animal weight. Tumor and organ-associated radioactivity were expressed as percent injected dose per total organ weight (%ID/g). Data represents mean  $\pm$  SD;  $n = 8$ .

### 3.6. *In vivo* therapeutic efficacy of siARv<sup>m</sup>-LNP in mice bearing 22Rv1 xenografts

After determining the biodistribution of the siARv<sup>m</sup>-LNP in 22Rv1 tumor-bearing mice, the therapeutic efficacy of the siARv<sup>m</sup>-LNP system was tested against siARfl-LNP and siLUC-LNP in the same xenograft model. Once 22Rv1 tumors reached a size of 100 mm<sup>3</sup>, male NRG mice were randomly assigned into four groups treated with either PBS control, siARv<sup>m</sup>-LNP (5 mg/kg), siARfl-LNP (5 mg/kg), or siLUC-LNP (5 mg/kg). A total of 9 doses were administered through *i.v.* injection, once daily for the first 3 days and then twice per week (Fig. S3). Tumor volume was determined by caliper measurement throughout the study, and survival was defined as the time taken for tumors to reach a size of 1000 mm<sup>3</sup>. By day 14, siARv<sup>m</sup>-LNP treatment group showed a significant tumor growth inhibition relative to the PBS control while both siARfl-LNP and siLUC-LNP treatment groups did not (Fig. 6A). As shown by the survival curve in Fig. 6B, the siARv<sup>m</sup>-LNP treated 22Rv1 tumor-bearing mice showed higher survival rate (64%) compared to the siARfl-LNP (50%) and siLUC-LNP (46%) groups, which correlated to the reduced tumor burden from the therapeutic effect of AR knockdown. Interestingly, the siARfl- and siLUC-LNPs had an influence on the survival rate, albeit to a lesser degree than siARv<sup>m</sup>-LNP (Table S3). This *in vivo* result correlated with the non-specific toxicity of siARfl-LNP and siLUC-LNP against 22Rv1 cells, again suggesting a potential hypersensitivity treatment response to the 22Rv1 cell or targeting effect not specific to the AR protein. Nonetheless, the observations indicated that siARv<sup>m</sup>-LNP exhibited antitumor activity that was superior to siARfl-LNP and the negative siLUC-LNP control. Lastly, no substantial changes in the body weights of mice during the treatment, except when the body weights of the siARv<sup>m</sup>-LNP-treated mice dropped (<20%) after the first three doses was observed (Fig. 6C). Despite the initial reduction in body weight, the average body weight showed recovery by day 12 even after bi-weekly repeated dosing. The siARfl-LNP and siLUC-LNP treatment groups did not exhibit similar losses in weight, implying the effects were siARv<sup>m</sup>-LNP specific and may relate to AR-V7 knockdown.

To determine whether the tumor growth inhibition and animal survival were correlated to the target gene knockdown, tumors were excised at day 20 post-treatment, and RNA was extracted. AR transcript levels after administration of siARv<sup>m</sup>, siARfl, or siLUC-LNPs were determined by RT-qPCR. We observed that the siARv<sup>m</sup>-LNP treatment

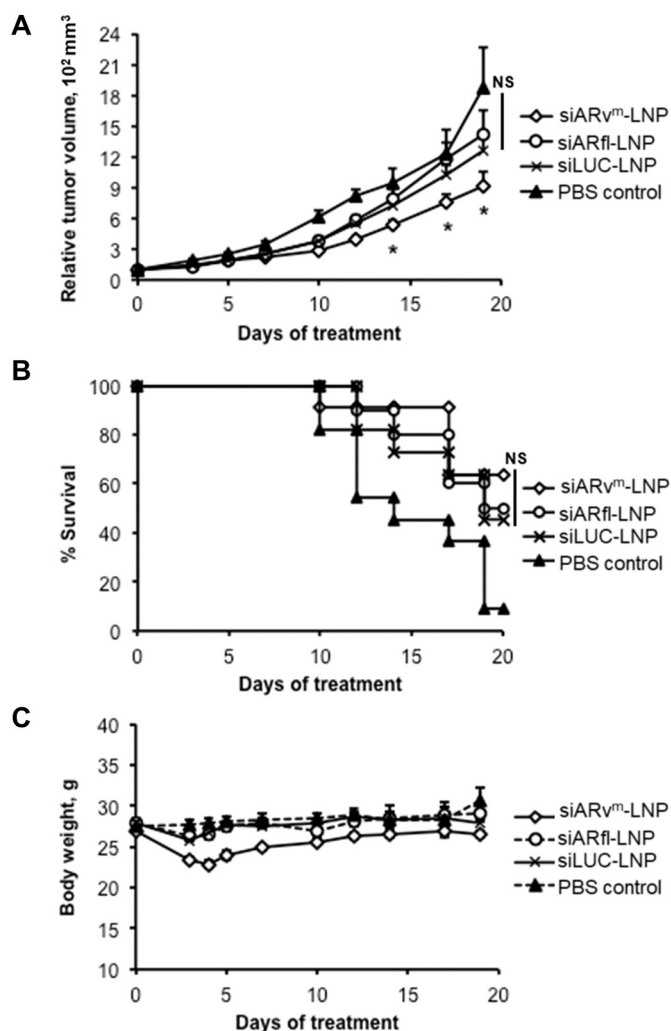


**Fig. 6.** Treatment of 22Rv1 xenografted mice with siARv<sup>m</sup>-LNP inhibited tumor growth and improved survival rate. Mice were inoculated subcutaneously with 22Rv1 cells. Once tumors reached 100 mm<sup>3</sup>, mice were randomly assigned into four groups treated with either PBS control, siARv<sup>m</sup>-LNP, siARf1-LNP, or siLUC-LNP (5 mg/kg). Injections were administered i.v. once daily for 3 days and then two times per week thereafter. (A) The mean relative tumor volume  $\pm$  SEM;  $n \geq 10$ , (B) survival rate, (C) and average body weight  $\pm$  SEM;  $n \geq 10$  was compared between the four groups, with survival defined as the time taken for tumors to reach 1000 mm<sup>3</sup>. \*  $p$ -value  $\leq 0.05$  siARv<sup>m</sup>-LNP compared with PBS control and NS indicated no significant difference between the three control groups (PBS control, siLUC-LNP and siARf1-LNP).

group exhibited significantly reduced AR transcript levels compared to the siLUC-LNP control group. In contrast, the siARf1-LNP-treated tumors did not show any significant difference in the AR mRNA abundance (Fig. S4A). No significant difference in the AR-V7 and PSA mRNA levels between the three siRNA-LNPs were observed (Fig. S4B and S4C). Despite successful AR and AR-V7 mRNA knockdown in 22Rv1 cells, the effects did not fully translate into a more complex *in vivo* model. Tumor size, tumor biology, dosing regime and the timeline at which the mRNA was extracted and measured could all be contributing factors to these findings. Nevertheless, the antitumor properties of siARv<sup>m</sup>-LNP were apparent and further investigation into siRNA-mediated cleavage of WT AR and variant AR-V7 mRNA as a potential therapeutic is warranted, especially in advanced stage ADT-resistant prostate cancers.

#### 4. Discussion

In this work, we demonstrate the efficacy of an LNP carrier of AR

variant-targeted siRNA (siARv) as an agent for down-regulating the AR-dependent growth of advanced prostate cancers. One area that requires further discussion is the correlation between *in vitro* and *in vivo* results, including the observation that non-specific effects appear to lead to some limited efficacy *in vivo* of formulations containing non-target siRNA. Secondly, we also discuss whether the therapeutic efficacy is limited by the lack of siRNA-LNP reaching the tumor site and propose ways in which the therapeutic potential of these siRNA-LNP systems targeting AR splice variants could be improved.

*In vitro*, the siARv<sup>m</sup> sequence identified had similar mRNA silencing capacity in both the LNCaP and the 22Rv1 prostate cancer cell lines. These trends extended through to PSA levels and showed therapeutic effects through the RNAi induced cell toxicity in 22Rv1 cells, which suggested that siARv<sup>m</sup> could be an effective therapeutic against advanced-stage prostate cancers. The *in vivo* results are consistent with siARv<sup>m</sup>-LNP having a greater impact on tumor growth than LNP systems containing siARf1 or siLUC; however, both siARf1 and siLUC showed positive effects compared to the PBS control. The non-specific response was also observed through the *in vitro* cell viability experiments, where at high doses (10  $\mu$ g/mL) the 22Rv1 cell line had a non-specific cytotoxic response from the control formulation in comparison to the LNCaP and PC3 cell lines. We speculate that this could be a result of either the 22Rv1 cells activating an innate immune stimulatory response toward the siRNA motifs [31] or non-target mRNA cleavage mediated by these siRNA [32]. Further investigation for expression profiling of siRNAs will clarify our understanding of the potential off-target effects, and whether altered siRNA design can mitigate these effects. Despite LNPs being initially designed as a delivery system, they may also act as an epigenetic factor and induce material-specific responses in certain cell lines. This has been previously observed in other transfection agents such as Lipofectin and Oligofectamine. Those agents have shown to affect gene expression that induces cell proliferation, differentiation, and apoptosis [33] and can significantly vary across different cell lines [34]. Previous studies that utilized these LNP systems for treatment of LNCaP-derived xenografts did not report similar effects of control LNPs on cell viability or tumor volume [18–20], which highlight that the siLUC-LNP effect we observed is likely to be cell line-specific. The underlying cause of such 22Rv1 susceptibility remain unknown and whether this is caused by the siRNA payload or the lipid components in the LNP system also warrant further investigation.

The next discussion concerns whether efficacy is limited by the lack of siRNA that reaches the tumor site. There are several physiological barriers that need to be overcome to systemically deliver the siRNA payload to the cytosol of tumor cells. Firstly, the siRNA-LNPs must have a long-circulation half-life that evade the rapid clearance from the mononuclear phagocyte system and leverage the EPR effect for tumor accumulation [35]. We used PEG-DSG and higher PEG lipid molar content to achieve the long *in vivo* circulation through minimizing interactions with opsonins and subsequent phagocytotic clearance. However, this does not resolve the issue with organ tropism caused by the ApoE-mediated endocytosis into hepatocytes, and it remains as a major challenge in the field of nanomedicine [36]. While the addition of PEG-DSG extended circulation half-life of these LNP, they are also less transfection potent in cells due to the less dissociative nature of the PEG lipid [20]. We also note that the number of LNPs that can extravasate from blood circulation and penetrate through a complex interstitial network of tumor-associated cells and extracellular matrix to reach cancer cells is also uncertain. The given total dose of 45 mg siRNA/kg (5 mg siRNA/kg  $\times$  9 i.v. injection) is significantly higher (9000 $\times$ ) than required to achieve an essentially complete gene silencing for target genes in the liver using similar LNP formulations [21]. It is likely that only a fraction of the siRNA ever reached the cytosol of target tumor cells given the lack of any specific targeting mechanism and the inaccessibility of the tumor to circulating LNPs. The fact that siRNA-LNP systems optimized for hepatocyte gene silencing are notably less potent for silencing target genes in other tissues also supports this



concept. These combined factors could be detrimental to the therapeutic effect of the siRNA-LNP that follows the current state-of-the-art design. Further formulation development is therefore essential to overcome the current challenges induced by the bio-nano-interaction for viable application in cancer therapy, an area of current investigation in our lab.

To tackle these hindrances to the development of siRNA mediated cancer gene therapy, we propose two potential approaches that could lead to more potent activity of siRNA-LNP at distal tumor sites. Firstly, improving the effective delivery to the tumor site is required. Concerning more effective delivery to tumor tissue, and to rectify the lack of transfection potency of the PEG-DSG due to the inhibited interactions with target cells, prostate-cancer targeting ligands could be incorporated/ligated onto the LNP surface; examples of such ligands are urea-based inhibitors for the prostate-specific membrane antigen. However, the benefits may be limited if the overall tumor accumulation remains low [18,19]. Other ongoing efforts include the alteration of lipid components and surface charges to redirect the LNPs to the targeted organs [37].

An alternative approach to improving tumor accumulation is to improve the tumor-specific transfection potency of siRNA-LNP systems. There are many efforts underway to achieve this, ranging from increasing the potency of the siRNA oligonucleotide, to improving the cytoplasmic delivery of the siRNA payload. In terms of the clinical development of siRNA-based therapies, there are several generations of modification motifs proven to enhance oligonucleotide knockdown potency [38]. Here, a single modification pattern was tested *in vitro* and carried forward, leaving room for improving the oligonucleotide potency *in vivo* based on a sequence modification approach. It is noted that the efficiency of currently “gold-standard” siRNA-LNP systems for intracellular delivery is estimated to be at most ~2% [39]. Approaches that enhance endosomal escape and cytosolic delivery of the LNP siRNA payload, such as the use of small-molecule antagonists to facilitate intracellular trafficking could potentially resolve this problem [40]. Another way to improve the effectiveness of the siArv<sup>m</sup>-LNP system is to combine it with chemotherapy that enables synergistic therapeutic effects. We have previously shown that stably incorporating taxane chemotherapeutic prodrugs in LNP-siRNA targeting AR induces additive therapeutic effects [41]. In addition, analysis of several clinical trials has concluded that combining docetaxel and anti-androgen therapies has a significant survival benefit in patients with advanced prostate cancer [42].

In conclusion, the scope of this research demonstrated that cell lines with varying AR, AR variant, and PSA expression could aid in the identification of potent siRNA oligonucleotides for the treatment of advanced prostate cancers. Furthermore, the consistent results in both *in vitro* and *in vivo* prostate cancer models identified siArv<sup>m</sup> as the most effective examined siRNA for inhibiting 22Rv1 xenograft tumor growth compared to LNPs containing siRNA targeting full-length AR (siARf) only or LNP containing a non-target oligonucleotide (siLUC). Thus, siArv<sup>m</sup>-LNP represents a promising potential treatment for advanced prostate cancers, requiring improvements in potency and specificity that are increasingly viable as both siRNA and LNP technologies advance.

## Contribution

J.Q performed all of the experiments, data analysis and wrote the manuscript. N-W, N.D-S performed the animal care for experiments as a part of the Investigational Drug Program at the BC Cancer Agency. M.H. Y-C, N-C and C.A.B contributed to the writing and editing of this manuscript. J.K performed the Cryo-EM imaging. R.v.d.M assisted in the tissue digestion. Y. Y. C. T conceived the project, planned the experiments and provided supervision. J.Q, D-W, and P.R.C conceived the project, planned the experiment, and interpreted the data.

## Credit author statement

J.Q: Conceptualization, Methodology, Software, Formal analysis. N-W, N.D-S: Methodology, Software. M.H.Y.C, N-C and C.A.B: Writing - Original Draft Preparation, Writing - Review & Editing. J.K: Methodology. R.v.d.M: Methodology. Y. Y. C. T: Conceptualization, Project administration, Funding acquisition, Supervision. D-W, and P.R.C: Conceptualization, Resources, Supervision, Project administration.

## Acknowledgements

The authors would like to acknowledge Nicole Wretham, Binab Karmacharya, Maryam Osooly, and Hong Yan, and the staff of the Investigational Drug Program at the BC Cancer Agency for their contributions to the xenograft biodistribution and efficacy studies. This work was supported by Prostate Cancer Canada grant D2013-5 and Canadian Institutes for Health Research grant FDN-148469. R.v.d.M's research on LNPs was supported by funding from the European Union's Horizon 2020 research and innovation program under the Marie Skłodowska-Curie grant agreement No. 660426 and a Veni STW Fellowship (#14385) from the Dutch Research Council (NWO). M.H.Y.C. acknowledges support from the NanoMedicines Innovation Network (NMN), a member of the Networks of Centres of Excellence Canada program.

## Appendix A. Supplementary data

Supplementary data to this article can be found online at <https://doi.org/10.1016/j.jconrel.2022.06.051>.

## References

- [1] National Cancer Institute, Cancer Stat Facts: Common Cancer Sites (n.d.), <https://seer.cancer.gov/statfacts/html/common.html>.
- [2] Canadian Cancer Society's Advisory Committee on Cancer Statistics, Can. Cancer Stat. (n.d.), <http://www.cancer.ca/Canadian-Cancer-Statistics-2017-EN.pdf>.
- [3] Y. Ceder, A. Bjartell, Z. Culig, M.A. Rubin, S. Tomlins, T. Visakorpi, The molecular evolution of castration-resistant prostate cancer, *Eur. Urol. Focus* 2 (2016) 506–513.
- [4] P.A. Watson, V.K. Arora, C.L. Sawyers, Emerging mechanisms of resistance to androgen receptor inhibitors in prostate cancer, *Nat. Rev. Cancer* 15 (2015) 701–711.
- [5] J.S. Sharp, A. Welti, J. Blagg, De Bono, Targeting androgen receptor aberrations in castration-resistant prostate cancer, *Clin. Cancer Res.* 129 (2016) 192–208.
- [6] D. Robinson, E.M. Van Allen, Y.-M. Wu, N. Schultz, R.J. Lonigro, J.-M. Mosquera, B. Montgomery, M.-E. Taplin, C.C. Pritchard, G. Attard, et al., Integrative clinical genomics of advanced prostate cancer, *Cell* 161 (2015) 1215–1228.
- [7] Z. Guo, X. Yang, F. Sun, R. Jiang, D.E. Linn, H. Chen, H. Chen, X. Kong, J. Melamed, C.G. Tepper, et al., A novel androgen receptor splice variant is up-regulated during prostate cancer progression and promotes androgen depletion-resistant growth, *Cancer Res.* 69 (2009) 2305–2313.
- [8] F. Antonarakis, E.S. Chandhasin, C. Osbourne, E. Luo, J. Sadar, M.D. Perabo, Targeting the N-terminal domain of the androgen receptor: a new approach for the treatment of advanced prostate cancer, *Oncologist* 21 (2016) 1427–1435.
- [9] M.D. Sadar, Small molecule inhibitors targeting the ‘Achilles’ heel of androgen receptor activity, *Cancer Res.* 71 (2011) 1208–1213.
- [10] C.A. Banuelos, I. Tavakoli, A.H. Tien, D.P. Caley, N.R. Mawji, Z. Li, Y.C. Jun Wang, Y. Yang, L. Imamura, J.G. Yan, R.J. Wen, M.D. Sadar Andersen, Sintokamide A is a novel antagonist of androgen receptor that uniquely binds activation function-1 in its amino-terminal domain, *J. Biol. Chem.* 291 (2016) 22231–22243.
- [11] C. Maurice-Dror, R. Le Moigne, U. Vaishampayan, R.B. Montgomery, M.S. Gordon, N.H. Hong, L. DiMascio, F. Perabo, K.N. Chi, A phase 1 study to assess the safety, pharmacokinetics, and anti-tumor activity of the androgen receptor n-terminal domain inhibitor epi-506 in patients with metastatic castration-resistant prostate cancer, *Investig. New Drugs* 40 (2021) 322–329.
- [12] R. Wilson, J.A. Doudna, Molecular mechanisms of RNA interference: a biological view of RNA interference • small regulatory RNAs in cellular function and dysfunction HHS public access, *Annu. Rev. Biophys.* 42 (2013) 217–239.
- [13] I.J. McEwan, Intrinsic disorder in the androgen receptor: identification, characterisation and drugability, *Mol. Biosyst.* 8 (2012) 82–90.
- [14] T.M. Allen, P.R. Cullis, Liposomal drug delivery systems: from concept to clinical applications, *Adv. Drug Deliv. Rev.* 65 (2013) 36–48.
- [15] M. Jayaraman, S.M. Ansell, B.L. Mui, Y.K. Tam, J. Chen, X. Du, D. Butler, L. Eltepu, S. Matsuda, J.K. Narayanannair, et al., Maximizing the potency of siRNA lipid nanoparticles for hepatic gene silencing in vivo, *Angew. Chem. Int. Ed. Engl.* 51 (2012) 8529–8533.

- [16] S.C. Semple, A. Akinc, J. Chen, A.P. Sandhu, B.L. Mui, C. Cho, D.W. Sah, D. Stebbing, E.J. Crosley, E. Yaworski, et al., Rational design of cationic lipids for siRNA delivery, *Nat. Biotechnol.* 28 (2010) 172–176.
- [17] A.V. Adams, D. Gonzalez-Duarte, A. O'Riordan, W.D. Yang, C.-C. Ueda, M. Kristen, I.H. Tournev, H. Schmidt, T. Coelho, J.L. Berk, et al., Patisiran, an RNAi therapeutic, for hereditary transthyretin amyloidosis, *N. Engl. J. Med.* 379 (2018) 11–21.
- [18] J.B. Lee, K. Zhang, Y.Y. Tam, Y.K. Tam, N.M. Belliveau, V.Y. Sung, P.J. Lin, E. LeBlanc, M.A. Ciufolini, P.S. Rennie, et al., Lipid nanoparticle siRNA systems for silencing the androgen receptor in human prostate cancer in vivo, *Int. J. Cancer* 131 (2012) 781–790.
- [19] J.B. Lee, K. Zhang, Y.Y. Tam, J. Quick, Y.K. Tam, P.J. Lin, S. Chen, Y. Liu, J.K. Nair, I. Zlatev, et al., A Glu-urea-Lys ligand-conjugated lipid nanoparticle/siRNA system inhibits androgen receptor expression in vivo, *Mol. Ther. Nucl. Acid* 5 (2016).
- [20] Y. Yamamoto, P.J.C. Lin, E. Beraldi, F. Zhang, Y. Kawai, J. Leong, H. Katsumi, L. Fazli, R. Fraser, P.R. Cullis, M. Gleave, siRNA lipid nanoparticle potently silences clusterin and delays progression when combined with androgen receptor cotargeting in enzalutamide-resistant prostate cancer, *Clin. Cancer Res.* 21 (2022) 4845.
- [21] S. Akinc, A. Zumbuehl, M. Goldberg, E.S. Leshchiner, V. Busini, N. Hossain, A. Bacallado, D.N. Nguyen, J. Fuller, R. Alvarez, et al., A combinatorial library of lipid-like materials for delivery of RNAi therapeutics, *Nat. Biotechnol.* 26 (2008) 561–569.
- [22] S. Chen, Y.Y.C. Tam, P.J.C. Lin, M.M.H. Sung, Y.K. Tam, P.R. Cullis, Lipid nanoparticles for delivery of nucleic acid therapeutics, *J. Control. Release* 235 (2016) 236–244.
- [23] Y. Li, M. Alsagabi, D. Fan, G.S. Bova, A.H. Tewfik, S.M. Dehm, Intragenic rearrangement and altered RNA splicing of the androgen receptor in a cell-based model of prostate cancer progression, *Cancer Res.* 71 (2011) 2108–2117.
- [24] L.L. Liu, N. Xie, S. Sun, S. Plymate, E. Mostaghel, X. Dong, Mechanisms of the androgen receptor splicing in prostate cancer cells, *Oncogene* 33 (2014) 3140–3150.
- [25] K.B.J.M. Cleutjens, C.C.E.M. Van Eekelen, H.A.G.M. Van Der Korput, A. O. Brinkmann, J. Trapman, Two androgen response regions cooperate in steroid hormone regulated activity of the prostate-specific antigen promoter, *J. Biol. Chem.* 271 (1996) 6379–6388.
- [26] M.A. Behlke, Chemical modification of siRNAs for in vivo use, *Oligonucleotides* 18 (2008) 305–320.
- [27] A.D. Judge, G. Bola, A.C.H. Lee, I. MacLachlan, Design of noninflammatory synthetic siRNA mediating potent gene silencing in vivo, *Mol. Ther.* 13 (2006) 494–505.
- [28] B. Cao, Y. Qi, G. Zhang, D. Xu, Y. Zhan, X. Alvarez, Z. Guo, X. Fu, S.R. Plymate, O. Sartor, H. Zhang, Y. Dong, Androgen receptor splice variants activating the full-length receptor in mediating resistance to androgen-directed therapy, *Oncotarget* 5 (2014) 1646–1656.
- [29] B. Cao, Y. Qi, Y. Yang, X. Liu, D. Xu, W. Guo, Y. Zhan, Z. Xiong, A. Zhang, A. R. Wang, X. Fu, H. Zhang, L. Zhao, J. Gu, Y. Dong, 20(S)-protopanaxadiol inhibition of progression and growth of castration-resistant prostate cancer, *PLoS One* 9 (2014) 26–28.
- [30] B.L. Mui, Y.K. Tam, M. Jayaraman, S.M. Ansell, X. Du, Y.Y.C. Tam, P.J.C. Lin, et al., Influence of polyethylene glycol lipid desorption rates on pharmacokinetics and pharmacodynamics of siRNA lipid nanoparticles, *Mol. Ther. Nucl. Acid* 2 (2013) 139.
- [31] Z. Meng, M. Lu, RNA interference-induced innate immunity, off-target effect, or immune adjuvant? *Front. Immunol.* 8 (2017) 1–7.
- [32] A.L. Jackson, P.S. Linsley, Noise amidst the silence: off-target effects of siRNAs? *Trends Genet.* 20 (2004) 521–524.
- [33] Y. Omid, A.J. Hollins, M. Benboubetra, R. Drayton, I.F. Benter, S. Akhtar, Toxicogenomics of non-viral vectors for gene therapy: a microarray study of lipofectin- and oligofectamine-induced gene expression changes in human epithelial cells, *J. Drug Target.* 11 (6) (2003) 311–323.
- [34] Y. Omid, A.J. Hollins, R. Drayton, S. Akhtar, Polypropylenimine dendrimer-induced gene expression changes: the effect of complexation with DNA, dendrimer generation and cell type, *J. Drug Target.* 13 (7) (2005) 431–443.
- [35] R.K. Jain, T. Stylianopoulos, Delivering nanomedicine to solid tumors, *Nat. Rev. Clin. Oncol.* 7 (2010) 653.
- [36] J. Shi, P.W. Kantoff, R. Wooster, O.C. Farokhzad, Cancer nanomedicine: progress, challenges and opportunities, *Nat. Rev. Cancer* 17 (2017) 20–37.
- [37] Q. Cheng, T. Wei, L. Farbiak, L.T. Johnson, S.A. Dilliard, D.J. Siegwart, Selective organ targeting (SORT) nanoparticles for tissue-specific mRNA delivery and CRISPR-Cas gene editing, *Nat. Nanotechnol.* 15 (2020) 313–320.
- [38] Y. Huang, Preclinical and clinical advances of GalNAc-decorated nucleic acid therapeutics, *Mol. Ther. Nucl. Acid* 6 (2017) 116–132.
- [39] L. Sahay, G. Querbes, W. Alabi, C. Eltoukhy, A. Sarkar, S. Zurenko, C. Karagiannis, E.K. Chen, D. Zoncu, et al., Efficiency of siRNA delivery by lipid nanoparticles is limited by endocytic recycling, *Nat. Biotechnol.* 31 (2013) 653.
- [40] H. Wang, Y.Y. Tam, S. Chen, J. Zaifman, R. van der Meel, M.A. Ciufolini, P. R. Cullis, The Niemann-pick C1 inhibitor NP3.47 enhances gene silencing potency of lipid nanoparticles containing siRNA, *Mol. Ther.* 24 (2016) 2100–2108.
- [41] R. van der Meel, S. Chen, J. Zaifman, J.A. Kulkarni, X.R.S. Zhang, Y.K. Tam, M. B. Bally, R.M. Schiffelers, M.A. Ciufolini, P.R. Cullis, Y.Y.C. Tam, Modular lipid nanoparticle platform technology for siRNA and lipophilic prodrug delivery, *Small* 17 (2021).
- [42] M. Tucci, V. Bertaglia, F. Vignani, C. Buttiglieri, C. Fiori, F. Porpiglia, G. V. Scagliotti, M. Di Maio, Addition of docetaxel to androgen deprivation therapy for patients with hormone-sensitive metastatic prostate cancer: a systematic review and meta-analysis, *Eur. Urol.* 69 (2016) 563–573.